Journal of Materials Chemistry B

PAPER

View Article Online
View Journal | View Issue

Published on 03 March 2016. Downloaded by University of South Carolina Libraries on 14/12/2016 21:30:48.

Cite this: J. Mater. Chem. B, 2016, 4, 2421

Surface labeling of enveloped virus with polymeric imidazole ligand-capped quantum dots *via* the metabolic incorporation of phospholipids into host cells†

Xia Zhao,‡[a] Yi Shen,‡[b] Enoch A. Adogla,[b] Anand Viswanath,[b] Rui Tan,[b] Brian C. Benicewicz,[b] Andrew B. Greytak,*[b] Yuan Lin[a] and Qian Wang[b]

Received 29th January 2016,
Accepted 3rd March 2016

DOI: 10.1039/c6tb00263c

www.rsc.org/MaterialsB

We report a general method for the preparation of quantum dot-labeled viruses through a strain-promoted azide–alkyne cycloaddition (SPAAC) reaction. The quantum dot sample was functionalized with methacrylate-based polymeric imidazole ligands (MA-PILs) bearing dibenzocyclooctyne groups. Enveloped measles virus was labeled with azide groups through the metabolic incorporation of a choline analogue into the host cell membrane, and then linked with the modified QDs. The virus retained its infectious ability against host cells after the modification with MA-PIL capped QDs.

Introduction

Quantum dots (QDs) are emerging as attractive candidates in biolabeling applications due to their greater excitation cross-sections and better photostability.[1–4] QDs synthesized with hydrophobic ligand coatings can be made bio-compatible *via* exchange reactions with hydrophilic ligands bearing nucleophilic anchoring groups such as thiol and amine.[5–7] This strategy has shown a smaller hydrodynamic radius than is achieved by alternative encapsulation strategies in which the initial ligand coating is retained.[4,8] In order to improve the long term stability of QDs in water, several groups have explored the use of multiple binding (multidentate) polymeric ligands instead of traditional mono- and di-thiol based ligands.[6,9–13] One promising class of polymeric ligands utilizes imidazoles as anchoring groups. Krull's group has used such polymeric imidazole ligand (PIL) capped QDs as fluorescence resonance energy transfer (FRET) donors for biosensors;[14,15] Bawendi's group and Mattoussi's group have shown that PIL-capped QDs can be used to label cells and their brightness can be maintained over an extended time.[6,10] Cai's group has used PIL-capped QDs to label viruses and shown that the viruses maintain their infectivity both *in vitro* and *in vivo*;[9,16] however, in this case the PILs were prepared by the direct modification of poly(maleic anhydride), which leaves residual carboxylic acid side chains that may influence the overall charge of QDs after a ligand exchange reaction. Recently, a new method for the preparation of methacrylate-based PILs (MA-PILs) with improved control of the composition and molecular weight has been introduced and has been shown to lead to water-soluble QDs that are compatible with live cell imaging.[17,18] A ternary copolymer version of the MA-PILs can incorporate PEG side chains for steric stabilization in water, imidazole anchoring groups, as well as primary amines that are available for further modification.[19]

Measles virus (MV) is a member of the morbillivirus subgroup of paramyxoviruses, containing glycosylated envelope proteins hemagglutinin (H) and fusion (F) that are embedded in the phospholipid bilayer envelope.[20] Live attenuated MV has been shown to possess promising oncolytic activity against many tumor cells,[21,22] which enables the possibility of virotherapy for cancer treatment.[23] For the sake of virotherapy, it is urgent to develop labeling strategies for the site-specific modification of the virus surface with functional handles such as folate and folate receptor-specific antibody, which can achieve targeting to tumor cells while avoiding normal cells.[24] The surface modification of enveloped viruses in the literature has focused on both surface proteins and the phospholipid envelope. Because of the characteristic that viruses recognize their host cells by surface proteins, the covalent linkage of functionalities to surface proteins that is achieved by chemical modification,[9,25] genetic engineering[26] and metabolic incorporation of azido sugars[27,28] could affect the normal properties of viruses including their interaction with host cells. Since the virus envelope is derived from a host cell membrane,[29] the metabolic incorporation of phospholipids that carry functional groups into a host cell

[a] State Key Laboratory of Polymer Physics and Chemistry, Changchun Institute of Applied Chemistry, Chinese Academy of Sciences, Changchun 130022, P. R. China
[b] Department of Chemistry and Biochemistry, University of South Carolina, Columbia, South Carolina 29208, USA. E-mail: greytak@sc.edu

† Electronic supplementary information (ESI) available: Supporting figures. See DOI: 10.1039/c6tb00263c

‡ XZ and YS contributed equally to this manuscript.

Published on 03 March 2016. Downloaded by University of South Carolina Libraries on 14/12/2016 21:30:48.

membrane has enabled the subsequent modification of virus envelopes during virus replication and assembly.[30,31]

Importantly, because the native surface proteins will be preserved during the envelope modification, this approach should help virus infectivity to be maintained to the largest extent. Recently, Pang and coworkers have reported a simple and fast method to label pseudorabies virus with biotin by feeding the host cells with commercial 1,2-dioleoyl-*sn-glycero*-3-phosphoethanolamine-*N*-(cap biotinyl) (sodium salt) during virus replication.[32] In addition, Salic's group has demonstrated that synthetic choline analogues bearing azide or alkyne groups including azidoethyl-choline (AECho), azidopropyl-choline (APCho) and propargyl-choline can be incorporated into the phospholipids of cells and tissues.[33,34] Based on this, Xie *et al.* utilized AECho and APCho to achieve the surface functionalization of vaccinia virus *via* metabolic incorporation in host cells.[35]

Until now, there have been few examples of the use of QDs to label enveloped virus. Wang's group and Pang's group have utilized the streptavidin-conjugated QDs to modify the vesicular stomatitis virus and influenza virus successfully for the study of the tracking of labelled virus into host cells.[36–38] Similarly, Cai's group has labelled the enveloped baculovirus with PIL-capped QDs through copper-free click chemistry and maintained their infectivity.[9] Xie's group and Pang's group have also modified the vaccinia virus, influenza virus and vesicular stomatitis virus with the QDs that was functionalized by the direct modification of amine and carboxylic-acid functionalized QDs.[25,39,40] However, all of these studies use the genetic or chemical modification of surface protein to label the virus. Additionally, except for Cai's work, all the studies employed acyl transfer chemistry to install clickable handles on water soluble QDs with amine-bearing coatings. In such cases, the synthetic yield for functional group attachment may be limited due to competing interactions in the QD surface environment.[6]

In this work, we labeled a live attenuated MV envelope with azido groups by metabolically incorporating an azide-bearing choline analogue AECho into the MV phospholipid bilayer *via* host cells. Then the as-synthesized CdSe/CdZnS QDs are purified using a gel permeation chromatography (GPC) method[41] and are subsequently exchanged with dibenzocyclooctyne (DBCO) functionalized MA-PILs. The exchanged QDs (PIL-QDs-DBCO) are attached to the azide-labeled MV (N_3-MV) through a copper-free, strain-promoted azide–alkyne cycloaddition (SPAAC) reaction (Scheme 1). The QD-labeled MV maintains its infectious ability against host Vero cells. We believe that the present study demonstrates the feasibility of a metabolic labeling approach, and the viability and utility of a mild and reproducible method for membrane-enveloped virus labeling with QDs.

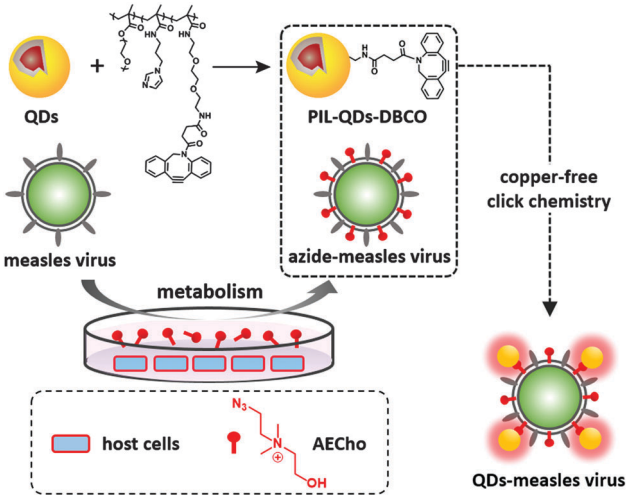

Scheme 1 Schematic illustration of the synthesis of PIL-QDs-DBCO, the azide labeling of measles virus assisted by host cells and the strategy for labeling virus with QDs *via* copper-free click chemistry.

Experimental section

Materials and analytical methods

Cadmium oxide (CdO; 99.999%), zinc oxide (ZnO; 99.999%), trioctylphosphine (TOP; 97%) and trioctylphosphine oxide (TOPO; 99%) were purchased from STREM Chemicals. Oleic acid (99%), 1-octadecene (ODE; 90% technical grade), and selenium (Se; 99.999%) were purchased from Alfa Aesar. Bio-Beads S-X1 GPC medium was obtained from BioRad Laboratories. Oleylamine (80–90%) and bis(trimethylsilyl) sulfide ($(TMS)_2S$; 95%) were purchased from Acros Organics. Rhodamine chloride 640 (R640) was obtained from exciton. Toluene (99.5% ACS analysis grade) was purchased from Mallinckrodt Chemicals. AIBN was purchased from Sigma Aldrich and recrystallized thrice from methanol. Poly(ethyleneglycol) methacrylate (500 g mol^{-1}) was obtained from Sigma Aldrich and was passed through a neutral alumina column to remove inhibitors before use. Measles virus (MV) and Vero cells were obtained from the U.S. Centers for Disease Control and Prevention (CDC). DBCO–NHS ester and DBCO-Fluor 488 were purchased from Click Chemistry Tools. All the other chemicals were purchased from Fisher and used as received. Procedures under nitrogen (N_2) or a vacuum environment were carried out using Schlenk line techniques or a glovebox.

Transmission electron microscopy (TEM) images were obtained using a Hitachi H-8000 microscope. Dynamic light scattering (DLS) was performed using a DynaPro-MSX instrument with a 690 nm laser wavelength (Wyatt Technology Corporation, Santa Barbara, CA). CellTiter-Blue cell viability assays were performed using a Tecan Infinite M200 microplate reader. Fluorescence images were obtained using a Carl Zeiss LSM 700 confocal laser scanning microscope. The absorption spectra of QDs were recorded using a Thermo Scientific Evolution Array UV-Visible Spectrophotometer, and the emission spectra were recorded using an Ocean Optics USB 4000 spectrometer under ~365 nm excitation.

Preparation of PIL-QDs-DBCO

The CdSe/CdZnS core/shell QDs were synthesized through a selective ionic adhesion and reaction (SILAR) method.[18] The growth process was monitored by absorption and emission spectra (Fig. S1, ESI†). Totally 9 monolayers of CdZnS shells

 This journal is © The Royal Society of Chemistry 2016

Published on 03 March 2016. Downloaded by University of South Carolina Libraries on 14/12/2016 21:30:48.

were coated onto the CdSe core. The MA-PIL ternary polymer was prepared as described previously,[19] which includes 40% imidazole for QD binding, 20% amine for post-modification and 40% PEG for water solubility. The number average molecular weight of the polymer was 33.5 kD and the polydispersity index (PDI) was 1.19. The PIL polymer was purified by dialysis and precipitation/redissolution, and then functionalized with DBCO by stirring the polymer with the DBCO–NHS ester (the polymer to DBCO mole ratio is 1 : 10) in a mixture of DMSO and chloroform (1 : 4) overnight (reaction scheme in Fig. S2, ESI†). The as-synthesized QDs were purified by one cycle of precipitation and redissolution followed by GPC purification in a toluene solvent. After this, the QDs were pumped dry and were mixed in the above DBCO–polymer solution (mole ration QD : polymer = 1 : 100). The mixture was stirred for 1 h, after which 0.5 mL of methanol was injected into the solution and stirring was continued for another 30 min. The resulting PIL-QDs-DBCO were precipitated by hexane and ethanol and redispersed by phosphate buffer saline (PBS). The water soluble dots were further purified by dialysis and were filtered using a 0.2 μm membrane.

Azide dye labeling on the PIL-QDs-DBCO

One set of PIL-QDs-DBCO was dialysed and mixed with an excess amount of a 3-azidocoumarin dye (MW = 437.4, a ratio of the dye to QDs is close to 200 : 1) in water. The mixture was stirred vigorously for 3 min and then dialyzed 4000 times using a centrifugal filter (membrane cut-off: 50 kDa) to remove the unreacted dye molecules.

Quantum yield measurement

The quantum yield (QY) of the PIL-QDs-DBCO samples was measured relative to rhodamine 640 (R640, QY = 99% in ethanol). The fluorescence spectra of QD and the R640 dye were recorded under identical spectrometer conditions on a Varian fluorescence spectrometer in triplicate and averaged. The optical density was kept below 0.1 between 550 and 800 nm to avoid internal filtering effects. The QY was calculated based on the integrated intensities of the emission spectra, the absorption at the excitation wavelength and the refraction index of the solvent using the equation:

$$\mathrm{QY_{QDs}} = \mathrm{QY_{dye}} \times \frac{\mathrm{Absorbance_{dye}}}{\mathrm{Absorbance_{QDs}}} \times \frac{\mathrm{Emission\ integral_{QDs}}}{\mathrm{Emission\ integral_{dye}}} \times \frac{\mathrm{Refraction\ index_{water}}^2}{\mathrm{Refraction\ index_{ethanol}}^2}$$

The precision of this measurement in our case is limited by the precision of the absorbance measurement while the accuracy among samples in different solvents will be limited by the accuracy of the refractive index correction term.

Transmission electron microscopy imaging of PIL-QDs-DBCO

After purification, the PIL capped CdSe/CdZnS QD samples were brought into water to form a dilute solution (0.15 μM). One drop of the solution (~20 μL) was drop-cast on a clean TEM grid (400 mesh Ni grid with ultrathin carbon support film, Type-A, Ted Pella, Inc.). After allowing the sample to deposit on the grid for 30 min, the excess solution was wicked away using a tissue. The grids were then pumped dry under vacuum for 2 hours. The samples were then imaged using a microscope.

Cell culture and azide labeling

Vero cells were cultured in Dulbecco's modified Eagle's medium (DMEM, Hyclone) supplemented with 10% fetal bovine serum (FBS, Atlanta Biologicals), 100 IU per mL penicillin and 100 μg mL^{-1} of streptomycin (Hyclone). The azide labeling of Vero cells was achieved by cultivating cells in the DMEM containing certain concentrations of AECho. For fluorescence imaging, the azide-modified Vero cells were washed with PBS and were fixed with 4% (w/v) paraformaldehyde. Subsequently, cells were stained by 10 μM DBCO-Fluor 488 or 10 nM PIL-QDs-DBCO for 1 h, then washed with PBS. The nucleic acid of the cells was stained with 1 μg mL^{-1} DAPI for 10 min. After washing, the cells were imaged using a Carl Zeiss LSM 700 confocal laser scanning microscope imaging system. The PIL-QDs-DBCO was excited using a 555 nm laser, with fluorescence detected at 550–650 nm. DBCO-Fluor 488 was excited using a 488 nm laser, with fluorescence detected at 500–600 nm. The DAPI was excited using a 405 nm laser, with fluorescence detected at 420–500 nm.

Virus propagation and azide labeling

MV was propagated in a monolayer of Vero cells in the presence of 2% FBS. Generally, Vero cells were infected with wild type MV with a multiplicity of infection (MOI) of 0.1 pfu per cell. For azide-labeled MV (N_3-MV) propagation, the medium was supplemented with 400 μM AECho. The infected cells were scraped into medium 72 h post-infection and the cell debris was removed by centrifugation at 3000*g* for 15 min (4 °C). The control MV and N_3-MV were purified over a gradient of sucrose centrifuged at 30 000 rpm for 3 hours (4 °C).[42]

Virus titer assay

The titers of viruses were quantified by 50% tissue culture infective dose ($TCID_{50}$). Vero cells were cultured in 96-well plates in complete medium until the cells reached 80–90% confluence, followed by replacement of DMEM containing 2% FBS. The virus samples prepared in DMEM by 4-fold serial dilutions were added to Vero cells. After culture for 3 days, the cells were stained with 0.1% crystal violet and observed under an inverted microscope. The well number that had a cytopathic effect (CPE) on Vero cells was counted for the $TCID_{50}$ calculation according to the Reed and Muench method.[43]

One-step growth assay

Viruses were inoculated in the Vero cells monolayer at MOI of 0.2 pfu per cell for 8, 24, 48, 72, 84 and 96 h, respectively. At the end of each time point, the infected cells were scraped into medium and the cell debris was removed by centrifugation at 3000*g* for 15 min at 4 °C. The one-step growth curve of these viruses was titrated by $TCID_{50}$ on normal Vero cells according to a previous report.[44]

Published on 03 March 2016. Downloaded by University of South Carolina Libraries on 14/12/2016 21:30:48.

Transmission electron microscopy imaging of the virus

The morphology of the viruses was characterized using transmission electron microscopy (TEM). 5 μL of virus was dropped onto a carbon coated copper grid that pre-treated by 1% alcian blue for 5 min. After 10 min, unabsorbed virus was removed using a filter paper. Grids were fixed by 2% paraformaldehyde for 5 min; after that, 10 μL of 0.5% uranyl acetate was applied for 30 s. The samples were then observed using TEM.

Fluorescence co-localization assay

The purified MV or N_3-MV solution was dropped onto cover glasses for 1 h at 37 °C. Excess viruses were then washed away with PBS solution, and the remaining viruses were fixed with 3% paraformaldehyde for 30 min at room temperature. After being permeabilized with 0.5% Triton X-100 in PBS, the viruses were incubated with 10 μM DBCO-Fluor 488 for 1 h. The nucleic acid of the virus was stained with 10 μg mL^{-1} of propidium iodide (PI) for 15 min. Excess fluorophores were washed away with PBS. Fluorescence images were acquired using a Carl Zeiss LSM 700 confocal laser scanning microscope imaging system. DBCO-Fluor 488 was excited using a 488 nm laser, with emission detected at 500–600 nm. PI was excited using a 555 nm laser, with emission detected at 560–700 nm.

Fluorescence imaging of cells exposed to QD-labeled virus

QD-labeled MV was prepared by incubating the N_3-MV with 10 nM PIL-QD-DBCO. Vero cells were cultured in a 24-well plate at 1×10^5 cells per mL density. Then the cells were incubated with the as-prepared QD-labeled MV for 24 h at 37 °C to allow virus binding, the unbound viruses were removed by washing with PBS. The nucleic acid of the cells was stained with 1 μg mL^{-1} DAPI solution for 10 min, after which the cells were imaged using a Carl Zeiss LSM 700 confocal laser scanning microscope imaging system. QDs were excited using a 555 nm laser, with emission detected at 550–650 nm. DAPI was excited using a 405 nm laser, with emission detected at 420–500 nm.

Cell viability assay

Cell viability was determined by using CellTiter-Blue Cell Viability Assay Kit (Promega). Vero cells were incubated with AECho or PIL-QDs-DBCO at certain concentrations for 24 h, followed by the addition of a 10% CellTiter-Blue Assay reagent and incubation for 2 h. The fluorescence intensity was measured at 560/590 nm (Ex/Em) using a Tecan Infinite M200 microplate reader. Cells treated with only medium were considered 100% viable.

Results and discussion

The QDs were prepared by a selective ionic layer adhesion reaction (SILAR) method as described previously, and in total, 9 monolayers of CdZnS shell were grown to achieve the desired emission wavelength. The formation of the shell was monitored by the absorption and emission spectra of the aliquot taken during the growth (Fig. S1, ESI†). The QDs were purified by GPC and then functionalized with the DBCO-containing MA-PIL polymer (Fig. S2, ESI†). In order to confirm the ligand-exchanged QDs that can be used to label the virus through the SPAAC reaction, an azido dye was introduced to a purified PIL-QDs-DBCO solution. As shown in Fig. S3 (ESI†), the absorption feature of the azido dye can be observed after a series of dialysis processes, which confirms that the DBCO group has been successfully attached to the QDs and maintains its reactivity toward organic azides. As shown in Fig. 1A, after surface modification, the QD sample maintained its absorption and emission features. According to TEM, the PIL-QDs-DBCO remained their monodispersity and narrow size distribution in PBS (pH = 7.4) without any visible indication of coalescence (Fig. 1B). The sample remained stable for more than 6 months when stored in a refrigerator at 4 °C, which maintained its quantum yield at 19% (Fig. S4, ESI†) and a hydrodynamic radius at around 17.3 nm with minimal aggregation based on DLS measurements (Fig. S5, ESI†). The toxicity of PIL-QDs-DBCO was detected by cell viability assay, which indicated the absence of cytotoxicity to Vero cells (Fig. S6, ESI†).

The choline analogue azidoethyl-choline (AECho) was synthesized following the reported procedure.[34] Vero cells were used as host cells for MV propagation and were grown in complete DMEM supplemented with AECho at certain concentrations. After co-incubation with AECho for 48 h, the Vero cells were fixed and stained with DBCO-Fluor 488 *via* the SPAAC reaction. As shown in Fig. S7 (ESI†), AECho was shown to biosynthetically bond to phospholipid and metabolically incorporate into the host cells. Cells showed strong fluorescence that was directly proportional in intensity to the AECho concentration. Moreover, the staining of azide-labeled Vero cells with PIL-QDs-DBCO showed a strong fluorescence signal of QDs on the cell membrane, demonstrating the successful incorporation of the azido group into the cell membrane (Fig. 2B). In contrast, PIL-QDs-DBCO applied to normal cells showed a nearly complete absence of binding. Since we did not observe any nonspecific binding with the imidazole-PEG copolymer coated QDs,[17] we conclude that the small (but non-zero) amount of non-specific binding here is due to the interaction between the cell surface and the DBCO/amine group. The cell viability could be kept above 90% when incubated with AECho at 600 μM for 48 h, indicating its biocompatibility (Fig. 2A). To achieve azide labeling of the MV envelope, viruses were propagated on azide-labeled Vero cells incubated with 400 μM AECho. The progeny viruses that are grown in AECho-treated Vero cells

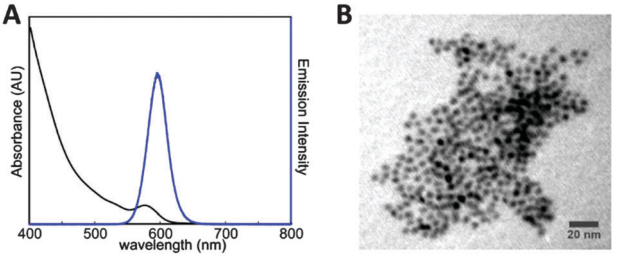

Fig. 1 (A) The absorbance (black) and emission (blue) spectra of PIL-QDs-DBCO in PBS. (B) TEM image of PIL-QDs-DBCO in aqueous solution. Scale bar indicates 20 nm.

 This journal is © The Royal Society of Chemistry 2016

Published on 03 March 2016. Downloaded by University of South Carolina Libraries on 14/12/2016 21:30:48.

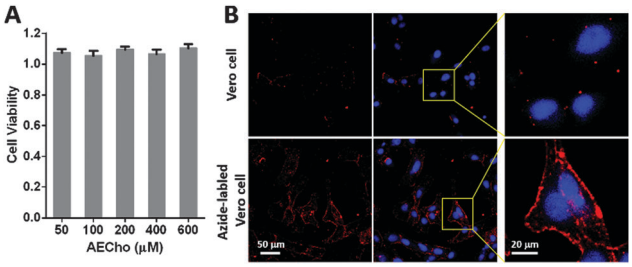

Fig. 2 (A) CellTiter-Blue viability assay of Vero cells incubated with AECho at different concentrations for 24 h. (B) Fluorescence imaging of azide-labeled Vero cells stained with PIL-QDs-DBCO (red) and DAPI (blue). Scale bars indicate 50 μm of regular views and 20 μm of enlarged views.

should be propagated with azido groups incorporated into their envelope upon release from their host cells, producing the azide-labeled MV (N_3-MV). The N_3-MVs were purified from the cell culture medium on a 20–60% sucrose gradient.[42] To evaluate the production of N_3-MV, $TCID_{50}$ of viruses was detected based on the Reed–Muench formula.[43] The data showed that control MV and N_3-MV were at a comparable titer of around 10^6 $TCID_{50}$ mL^{-1}, suggesting that metabolic labeling did not affect the propagation of MV in host Vero cells (Fig. 3A). The infectivity of N_3-MV was evaluated by one-step growth kinetics.[44] As shown in Fig. 3B, the N_3-MV reached 2×10^5 $TCID_{50}$ mL^{-1} at 96 h post-infection, which did not indicate a statistically significant difference from that of control MV. In addition, the N_3-MV retained the intact structure of the control virus (Fig. 3C). These results suggested that the azide labeling *via* metabolic incorporation of choline analogue AECho did not disturb virus production or infectivity.

A co-localization assay was performed to evaluate if the N_3-MV could indeed be functionalized *via* the SPAAC reaction. The viruses were overlaid on coverslips for 60 min at 37 °C, then fixed, permeabilized, and were stained with both DBCO-Fluor 488 for the azido group and propidium iodide (PI) for nucleic acid.

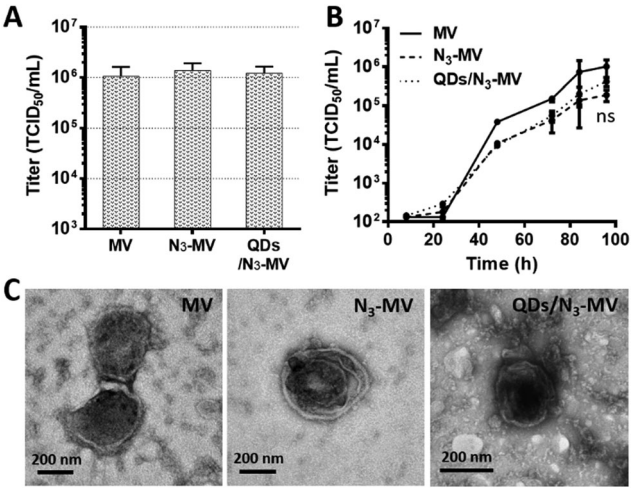

Fig. 3 (A) Production of control MV, N_3-MV and QDs/N_3-MV. (B) One-step growth curves of control MV, N_3-MV and QDs/N_3-MV. ns = not significant. (C) TEM images of control MV, N_3-MV and QDs/N_3-MV. Scale bars indicate 200 nm.

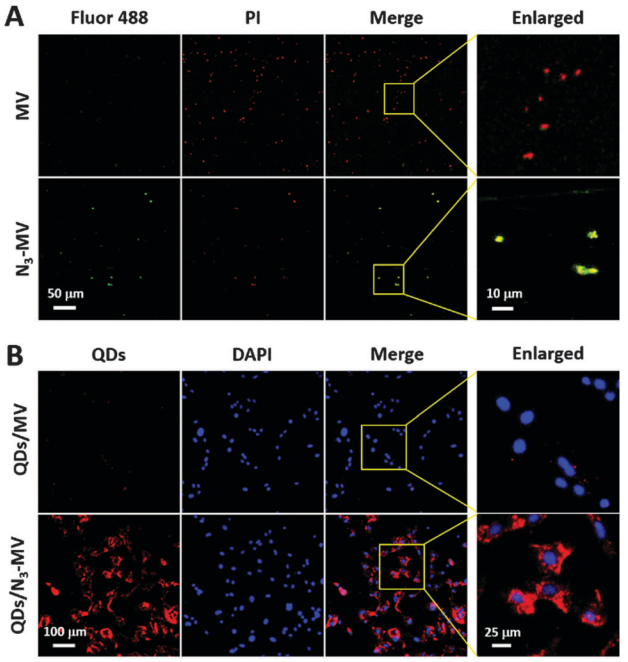

Fig. 4 (A) Fluorescence imaging of control MV and N_3-MV stained with DBCO-Fluor 488 (green) and propidium iodide (red). Scale bars indicate 50 μm of regular views and 10 μm of enlarged views. (B) Fluorescence imaging of Vero cells co-incubated with QDs-labeled MV (red, QDs; blue, DAPI labeled cell nucleic acid). Scale bars indicate 100 μm of regular views and 25 μm of enlarged views.

The fluorescence imaging results showed that most of the fluorescence signals of PI co-localized with that of Fluor 488 for N_3-MV, appearing as yellow in a merged image. In contrast, there was no Fluor 488 signal observed for the control MV (Fig. 4A). Therefore, it was further verified that virus produced from azide-labeled Vero cells had azido groups incorporated into the virus surface, which were available for further chemical modification with DBCO derived functionalities through the SPAAC reaction.

Next, we labeled the azide modified virus with PIL-QDs-DBCO, followed by co-incubating with a new set of Vero host cells. The virus activity and infectivity after being conjugated with QDs were comparable to those of the virus before modification (Fig. 3A and B, detail in Fig. S8, ESI†). As shown in Fig. 3C, the virus maintained its intact structure after QD labeling, which is consistent with the biological result. In a higher magnification TEM image of the QD labelled virus, several QDs could be observed on the virus surface (Fig. S9, ESI†). The fluorescence imaging of the new Vero host cells exposed to QD-labeled MV showed a remarkably prominent signal of QDs on the cell membrane, indicating that QDs-labeled MV could interact with Vero cells. On the contrary, there was no signal of QDs when the cells were co-incubated with a mixture of control MV and PIL-QDs-DBCO, suggesting that nonspecific adsorption of the PIL-QDs-DBCO on the cell surface is absent (Fig. 4B), and that the signal observed for QD-labeled MV is indeed indicative of bond formation between the N_3-MV and the PIL-QDs-DBCO.

Combining the preserved virus activity and infectivity, the interaction between QDs-labeled MV and Vero cells demonstrates

Published on 03 March 2016. Downloaded by University of South Carolina Libraries on 14/12/2016 21:30:48.

that the covalent attachment of QDs onto N_3-MV did not compromise the infectious ability of the virus against host cells.

Conclusions

In summary, we have proposed a mild and reproducible method for the preparation of QD-labeled viruses. We demonstrated that enveloped MV could be metabolically labeled with a choline analogue AECho assisted by host cells. The azide incorporation into the viral envelope did not affect the production and activity of progeny N_3-MV. The QDs can be functionalized with a DBCO-bearing methacrylate-based polymeric imidazole ligand, and subsequently maintain brightness and colloidal stability for more than 6 months. The QDs and virus can be linked together through a SPAAC reaction without the addition of a copper catalyst, and the infectious ability of virus does not change. The remarkable ease of this metabolic labeling approach makes it accessible to other membrane-enveloped viruses, and the MA-PIL capped QDs have also been proven to be a reliable bio-imaging probe. It is envisaged that this labeling strategy will greatly facilitate the development of new anticancer agents that can retarget oncolytic viruses specific to cancer cells for cancer virotherapy.

Acknowledgements

This work was supported by the National Natural Science Foundation of China (21429401 and 21374119), the US National Science Foundation (NSF CHE-1307319), and by the University of South Carolina, including an Aspire grant to ABG. XZ is grateful for the support of China Scholarship Council. YS acknowledges a Dean's Dissertation Fellowship from the USC College of Arts and Sciences. We thank Prof. Melissa A. Moss of USC for assistance with DLS measurements.

Notes and references

1 M. Bruchez, M. Moronne, P. Gin, S. Weiss and A. P. livisatos, *Science*, 1998, **281**, 2013–2016.
2 W. R. Algar, K. Susumu, J. B. Delehanty and I. L. Medintz, *Anal. Chem.*, 2011, **83**, 8826–8837.
3 J. Zhou, Y. Yang and C. Y. Zhang, *Chem. Rev.*, 2015, **115**, 11669–11717.
4 G. Palui, F. Aldeek, W. Wang and H. Mattoussi, *Chem. Soc. Rev.*, 2015, **44**, 193–227.
5 A. R. Clapp, E. R. Goldman and H. Mattoussi, *Nat. Protoc.*, 2006, **1**, 1258–1266.
6 W. Liu, A. B. Greytak, J. Lee, C. R. Wong, J. Park, L. F. Marshall, W. Jiang, P. N. Curtin, A. Y. Ting, D. G. Nocera, D. Fukumura, R. K. Jain and M. G. Bawendi, *J. Am. Chem. Soc.*, 2010, **132**, 472–483.
7 W. Liu, H. S. Choi, J. P. Zimmer, E. Tanaka, J. V. Frangioni and M. Bawendi, *J. Am. Chem. Soc.*, 2007, **129**, 14530–14531.
8 C. Schieber, A. Bestetti, J. P. Lim, A. D. Ryan, T. L. Nguyen, R. Eldridge, A. R. White, P. A. Gleeson, P. S. Donnelly, S. J. Williams and P. Mulvaney, *Angew. Chem., Int. Ed.*, 2012, **51**, 10523–10527.
9 P. Zhang, S. Liu, D. Gao, D. Hu, P. Gong, Z. Sheng, J. Deng, Y. Ma and L. Cai, *J. Am. Chem. Soc.*, 2012, **134**, 8388–8391.
10 W. Wang, X. Ji, A. Kapur, C. Zhang and H. Mattoussi, *J. Am. Chem. Soc.*, 2015, **137**, 14158–14172.
11 F. Aldeek, M. Safi, N. Zhan, G. Palui and H. Mattoussi, *ACS Nano*, 2013, **7**, 10197–10210.
12 M. Liras, I. Quijada-Garrido, M. Palacios-Cuesta, S. Munoz-Durieux and O. Garcia, *Polym. Chem.*, 2014, **5**, 433–442.
13 A. M. Smith and S. Nie, *J. Am. Chem. Soc.*, 2008, **130**, 11278–11279.
14 E. Petryayeva, W. R. Algar and U. J. Krull, *Langmuir*, 2013, **29**, 977–987.
15 E. Petryayeva and U. J. Krull, *Langmuir*, 2012, **28**, 13943–13951.
16 H. Pan, P. Zhang, D. Gao, Y. Zhang, P. Li, L. Liu, C. Wang, H. Wang, Y. Ma and L. Cai, *ACS Nano*, 2014, **8**, 5468–5477.
17 C. M. Johnson, K. M. Pate, Y. Shen, A. Viswanath, R. Tan, B. C. Benicewicz, M. A. Moss and A. B. Greytak, *J. Colloid Interface Sci.*, 2015, **458**, 310–314.
18 A. Viswanath, Y. Shen, A. N. Green, R. Tan, A. B. Greytak and B. C. Benicewicz, *Macromolecules*, 2014, **47**, 8137–8144.
19 A. Viswanath, P. Paudel, P. Kittikhunnatham, A. N. Green, A. B. Greytak and B. C. Benicewicz, *Polym. Chem.*, 2015, **6**, 7036–7044.
20 J. M. Hardwick and R. Bussell, *J. Virol.*, 1978, **25**, 687–692.
21 T. Nakamura and S. J. Russell, *Expert Opin. Biol. Ther.*, 2004, **4**, 1685–1692.
22 H. Lucie, K. Valerie, P. A. Oberholzer, K. Thomas, N. Hussein and D. Reinhard, *Blood*, 2005, **106**, 2287–2294.
23 K. Hasegawa, T. Nakamura, M. Harvey, Y. Ikeda, A. Oberg, M. Figini, S. Canevari, L. C. Hartmann and K. W. Peng, *Clin. Cancer Res.*, 2006, **12**, 6170–6178.
24 Y. Lu and P. S. Low, *J. Controlled Release*, 2003, **91**, 17–29.
25 J. Hao, L. L. Huang, R. Zhang, H. Z. Wang and H. Y. Xie, *Anal. Chem.*, 2012, **84**, 8364–8370.
26 S. Finke, K. Brzozka and K. K. Conzelmann, *J. Virol.*, 2004, **78**, 12333–12343.
27 X. Zhao, L. Cai, E. A. Adogla, H. Guan, Y. Lin and Q. Wang, *Bioconjugate Chem.*, 2015, **26**, 1868–1872.
28 P. S. Banerjee, P. Ostapchuk, P. Hearing and I. Carrico, *J. Am. Chem. Soc.*, 2010, **132**, 13615–13617.
29 H. Garoff, R. Hewson and D. J. E. Opstelten, *Microbiol. Mol. Biol. Rev.*, 1998, **62**, 1171–1190.
30 Y. H. Chen, C. H. Wang, C. W. Chang and C. A. Peng, *Integr. Biol.*, 2010, **2**, 258–264.
31 N. G. Mukherjee, L. L. Andrew and J. M. Le Doux, *Nanotechnology*, 2009, **20**, 065103.
32 B. H. Huang, Y. Lin, Z. L. Zhang, F. Zhuan, A. A. Liu, M. Xie, Z. Q. Tian, Z. Zhang, H. Wang and D. W. Pang, *ACS Chem. Biol.*, 2012, **7**, 683–688.
33 C. Y. Jao, M. Roth, R. Welti and A. Salic, *Proc. Natl. Acad. Sci. U. S. A.*, 2009, **106**, 15332–15337.
34 A. Salic, *US pat. Application*, 20120028290 A1, 2012.
35 L. L. Huang, G. H. Lu, J. Hao, H. Wang, D. L. Yin and H. Y. Xie, *Anal. Chem.*, 2013, **85**, 5263–5270.

 This journal is © The Royal Society of Chemistry 2016

Published on 03 March 2016. Downloaded by University of South Carolina Libraries on 14/12/2016 21:30:48.

36 K. I. Joo, Y. Lei, C. L. Lee, J. Lo, J. Xie, S. F. Hamm-Alvarez and P. Wang, *ACS Nano*, 2008, **2**, 1553–1562.
37 S. L. Liu, Z. L. Zhang, Z. Q. Tian, H. S. Zhao, H. Liu, E. Z. Sun, G. F. Xiao, W. Zhang, H. Z. Wang and D. W. Pang, *ACS Nano*, 2011, **6**, 141–150.
38 S. L. Liu, Z. Q. Tian, Z. L. Zhang, Q. M. Wu, H. S. Zhao, B. Ren and D. W. Pang, *Biomaterials*, 2012, **33**, 7828–7833.
39 L. L. Huang, Y. J. Jin, D. Zhao, C. Yu, J. Hao and H. Y. Xie, *Anal. Bioanal. Chem.*, 2014, **406**, 2687–2693.
40 Z. Y. Hong, C. Lv, A. A. Liu, S. L. Liu, E. Z. Sun, Z. L. Zhang, A. W. Lei and D. W. Pang, *ACS Nano*, 2015, **9**, 11750–11760.
41 Y. Shen, M. Y. Gee, R. Tan, P. J. Pellechia and A. B. Greytak, *Chem. Mater.*, 2013, **25**, 2838–2848.
42 W. J. Bellini, A. Trudgett and D. E. McFarlin, *J. Gen. Virol.*, 1979, **43**, 633–639.
43 L. J. Reed and H. Muench, *Am. J. Epidemiol.*, 1938, **27**, 493–497.
44 M. Kopp, B. G. Klupp, H. Granzow, W. Fuchs and T. C. Mettenleiter, *J. Virol.*, 2002, **76**, 8820–8833.